Trends in Photochemistry & Photobiology
Vol. 22, 2023

Original Article

Importance of emersion hour in microphytobenthos activity: a case of an intertidal mudflat

Marvin Meresse[1,2,3,4,*], François Gevaert[1,2,3,4], Gwendoline Duong[1,2,3,4] and Lionel Denis[1,2,3,4]

[1]Université de Lille, Unité Mixte de Recherche 8187 – Laboratoire d'Océanologie et de Géosciences, Station Marine de Wimereux, F-59000 Lille, France; [2]Centre National de la Recherche Scientifique, Unité Mixte de Recherche 8187 – Laboratoire d'Océanologie et de Géosciences, Station Marine de Wimereux, F-59000 Lille, France; [3]Université Littoral Côte d'Opale, Unité Mixte de Recherche 8187 – Laboratoire d'Océanologie et de Géosciences, F-62930 Wimereux, France; [4]Institut de Recherche pour le Développement, Unité Mixte de Recherche 8187 – Laboratoire d'Océanologie et de Géosciences, F-62930 Wimereux, France.

ABSTRACT

The intertidal zone is a dynamic habitat subject to constant tide fluctuations that provides a challenging and stressful environment for the organisms inhabiting it. As a microscopic primary producer living in association with benthic substrates, microphytobenthos play a crucial role and display adaptive characteristics like photoprotection, desiccation resistance, and migration behaviors. This vertical migration is an important adaptative mechanism that enables the microalgae constituting the microphytobenthos to optimize their light exposure and retreat into the sediments during low tide to avoid harsh conditions. Numerous studies have shown that these vertical migration mechanisms are governed by an internal clock, giving rise to endogenous rhythms. To better understand the microphytobenthic communities functioning, primary production is typically characterized through laboratory measurements, often performed independently of the photoperiod or/and tidal characteristics of the environment. However, the question arises: does the time of day and tidal phase have an impact on the processes measured? To investigate this, we simulated an artificial tidal cycle, creating four different scenarios to test the effects of 'day hour' and 'tidal phase moment'. During these scenarios, we used two complementary measurement tools: a pulse-amplitude modulated (PAM) fluorometer to assess surface microphytobenthic biomass and oxygen microsensors to obtain vertical distribution of photosynthetic activity. Our study, while confirming that the endogenous rhythm of microphytobenthos can be maintained for up to three days in the laboratory, shows that the intensity of vertical migratory rhythm varies with the day hour. Importantly, we have shown that the day hour significantly influences primary production estimates, with maximum production values potentially being up to three times higher when estimated during afternoon emersions compared to nocturnal emersions. In addition, the timing of measurements in relation to the immersion/emersion cycle can also have an impact on primary production estimates, and must be considered if reliable and realistic estimates are to be obtained.

KEYWORDS: internal clock, intertidal mudflat, microphytobenthos, migration behavior, modulated fluorescence, oxygen flux, photoregulation, primary production.

*Corresponding author: marvin.meresse@univ-lille.fr

1. Introduction

The intertidal zone, a dynamic and complex ecosystem situated between high and low tide levels along coastlines, encompasses a diverse range of coastal environments [1]. This unique habitat experiences changing environmental conditions, including variations in light, temperature, salinity, and nutrient availability [2]. Within this coastal ecosystem, microphytobenthos, primarily composed of algae [3-5] and cyanobacteria [6, 7], play a crucial role as primary producers [8] and major contributors to biodiversity and ecosystem functioning [5, 9, 10].

To ensure survival and prosperity in this dynamic environment, microphytobenthos have developed various adaptations. These adaptations include photoprotection mechanisms [11] to minimize damage from excessive light and UV radiation, strategies for desiccation resistance [12] to endure periods of emersion, and mechanisms for osmotic regulation to handle salinity variations [13, 14]. Through these adaptations, microphytobenthos efficiently utilize available resources and overcome environmental pressures. In addition to these adaptations, microphytobenthos in the intertidal zone employ a notable mechanism known as vertical migration. Microphytobenthos exhibit locomotion through the presence of a slit in their cell wall, enabling directional and reversible movement [15] supported by intricate micromovements [16], mainly to respond to ambient pressures [17]. Moreover, multiple research investigations have also presented convincing proof regarding the impact of an internal clock on the movement of microphytobenthos, showcasing the intricate relationship between their endogenous rhythm and migratory behavior [18-20]. The presence of an endogenous migratory behavior has been demonstrated through experiments that revealed consistent migration patterns, even in the absence of external physical synchronizers [21, 22]. Some studies have shown that microphytobenthos exhibit a distinct migratory behavior that is synchronized with the tidal and photoperiod cycles [22]. During daylight emersion, microphytobenthic cells move upward and form dense and temporary photosynthetic biofilms at the sediment surface, while they move back downward into deeper sediment layers before nighttime or immersion [22, 23] during which the microphytobenthos is darkened because of low light penetration in the water column. This rhythmic pattern is continuously adjusted to align with the daily and fortnightly tide timings, with longer or shorter tides between spring and neap tides, as well as the progressive changes in day length throughout the seasons. The purpose of vertical migration in microphytobenthos is to optimize their light exposure to maintain photosynthetic activity, as well as to utilize the physicochemical gradients within intertidal sediments [24, 25] in order to maintain productivity and resilience in response to the dynamic nature of the intertidal zone. By performing photosynthesis and carbon fixation in well-lit upper sediment layers, which are spatially disconnected from nutrient-rich, stable, and darker deeper layers where cell division takes place, these microphytobenthic cells can effectively exploit the resources available for their growth and survival [26]. Except for sandy sediments, where microphytobenthos have an epipsammic lifestyle [3, 27], the acquisition of motility is considered a crucial adaptation [23], enabling them to thrive in intertidal sediments. This way, by adjusting their vertical position within the sediment, microphytobenthos can adapt to the fluctuating intertidal conditions and ensure their survival in this challenging environment.

This understanding is pivotal in unraveling the mechanisms governing microphytobenthic activity. Through extensive research, scientists have delved into the interconnectedness of the endogenous rhythm and migratory patterns of microphytobenthos, shedding light on the coordination of physiological processes and ecological dynamics within intertidal ecosystems [3, 20, 25, 28]. But despite numerous studies on the internal clock of microphytobenthos, there are still uncertainties surrounding its mechanisms and implications. While the existence of an internal clock has been established, its precise regulation and interactions with other environmental factors remain under investigation. One significant knowledge gap lies in understanding the potential consequences of the rhythmic behavior driven by the internal clock on estimates of primary production in laboratory conditions. Therefore,

our study aimed to better understand the internal implications for accurate assessments of microphytobenthic primary production in laboratory experiments. This manuscript therefore presents a study in which the authors investigated the asynchrony of the tidal rhythm with what happens in the field, in order to study the impact of the internal clock on estimates of primary production in the laboratory. Thus, by understanding the internal clock effect on primary production estimations, we can refine our understanding of the ecological dynamics and functioning of microphytobenthic communities, contributing to more precise estimations of primary production in the intertidal zone.

2. Materials and Methods

2.1. Study site, sampling and sediment core conservation

The study was conducted on sediments sampled in the Canche estuary, located on the northern coast of France in the Eastern Channel. The sediment samples were collected on April 28, 2021, from the northern intertidal mudflat of the Canche estuary (50°32'07 "N and 1°35'45 "E). Due to its location in a macrotidal environment, the estuary is subject to tidal range of 8 meters during spring tides and 3 meters during neap tides, with a semi-diurnal tidal regime.

Prior to the experiment, three sediment cores with a diameter of 15 cm were collected during the night and stored in the dark until the early morning before sunrise. The sediment cores were transported to the laboratory and immersed in a bath of thermostatic bubbled seawater that corresponded to the immersion time of the site, in order to simulate the natural immersion conditions. This simulation was conducted in the dark to replicate the natural conditions, as preliminary measurements revealed that no light could reach the sediment during immersion due to the turbidity of the estuarine water column. One of the three cores was used for fluorescence and oxygen microprofiling, while the other two were used for sediment characterization. In this last two, to estimate the chlorophyll *a* (Chl *a*) concentrations in the topmost 0.5 centimeter of the wet sliced sediment thanks to the Lorenzen method [29], a total of three subcores of 2.6 cm inner diameter were randomly taken from each of the two sediment cores just prior to the acquisition sequence. Additionally, to determine the average sediment porosity, a total of 3 subcores were sampled in the two sediment cores and stored at -20 °C. The frozen subcores were manually sectioned into slices of various widths and then dried in an oven (60 °C) for a week [30, 31]. The porosity was calculated using the measured sediment water content, by weighing fresh and dry weights, and by assuming a dry particle density (ρ_{sed}) of 2.65 g.cm^{-3} [32] and a seawater density (ρ_w) of 1.03 g.cm^{-3}. The porosity was calculated using the following equation:

$$\varphi = \frac{\frac{W_w}{\rho_w}}{\frac{W_w}{\rho_w} + \frac{W_{sed}}{\rho_{sed}}} \quad (1)$$

where W_w and W_{sed} are the weight of water and sediment, respectively.

During the sampling, *in situ* measurements of surface sediment temperature and salinity were carried out by inserting a multi-parameter probe (HI9829, Hanna Instruments, France) into the first centimeter of sediment, located a few centimeters away from the core position.

In order to determine the maximum storage time for sediment core without any impact on sediment geochemistry, oxygen flux measurements were conducted under four different light intensities applied successively: (i) 0, (ii) 200, (iii) 475, and (iv) 1020 µmol.m^{-2}.s^{-1}. For each light intensity, 20 oxygen profiles were realized every day, over a period of 5 consecutive days.

Additionally, to assess any potential impact on sediment structure, 3 porosity measurements were performed successively before and after the study. To monitor the condition of the microphytobenthic communities, 3 daily measurements of Chl *a* concentration and F_v/F_m (see below) were conducted.

2.2. Simulating immersion/emersion in laboratory

2.2.1. Laboratory autonomous acquisition system of microphytobenthic activity data

To carry out the experimentation, an artificial tidal cycle was created in the laboratory to create

different scenarios. These scenarios took place at different times in relation to the tidal cycle, in order to determine the effect of the 'tidal moment' effect on primary production estimates with an emersion (i) before, (ii) during, (iii) at the beginning and (iv) ending with the theoretical immersion of the study site. These scenarios took place at different times of day in order to determine the effect of the 'time of day' effect on primary production estimates with an emersion at (i) 11:00, (ii) 01:00, (iii) 16:00, and (iv) 08:00. The study lasted for about three consecutive days, with 8-hour-long emersions and 6-hour-long immersions (Figure 1). During the emersion phases, fluorescence measurements and oxygen profiles were taken under increasing light levels.

An autonomous Photosynthetic-Irradiance (P-I) curve acquisition system was used. This system was presented and described by Meresse *et al.* [33]. This system is composed of two complementary tools: a microprofiling system with two oxygen microsensors (Ox-25, Unisense, Denmark) and a diving-PAM (Walz, Germany). This system has been placed in a climatic chamber (Fitoclima 600, Aralab, Portugal) which allows to work in controlled conditions thanks to the programming of the light intensity, temperature and hygrometry.

For each acquired P-I curve, a total of 14 light intensities were applied to the microphytobenthos, with light intensity ranging from 0 to 1650 $\mu mol.m^{-2}.s^{-1}$ (Figure 1). For each intensity, 8 profiles were made. These were obtained in pairs by using 2 microsensors at the same time. A vertical profile took 8 minutes to acquire which allowed us to obtain all the profiles necessary for the acquisition of a P-I curve in 07:30,

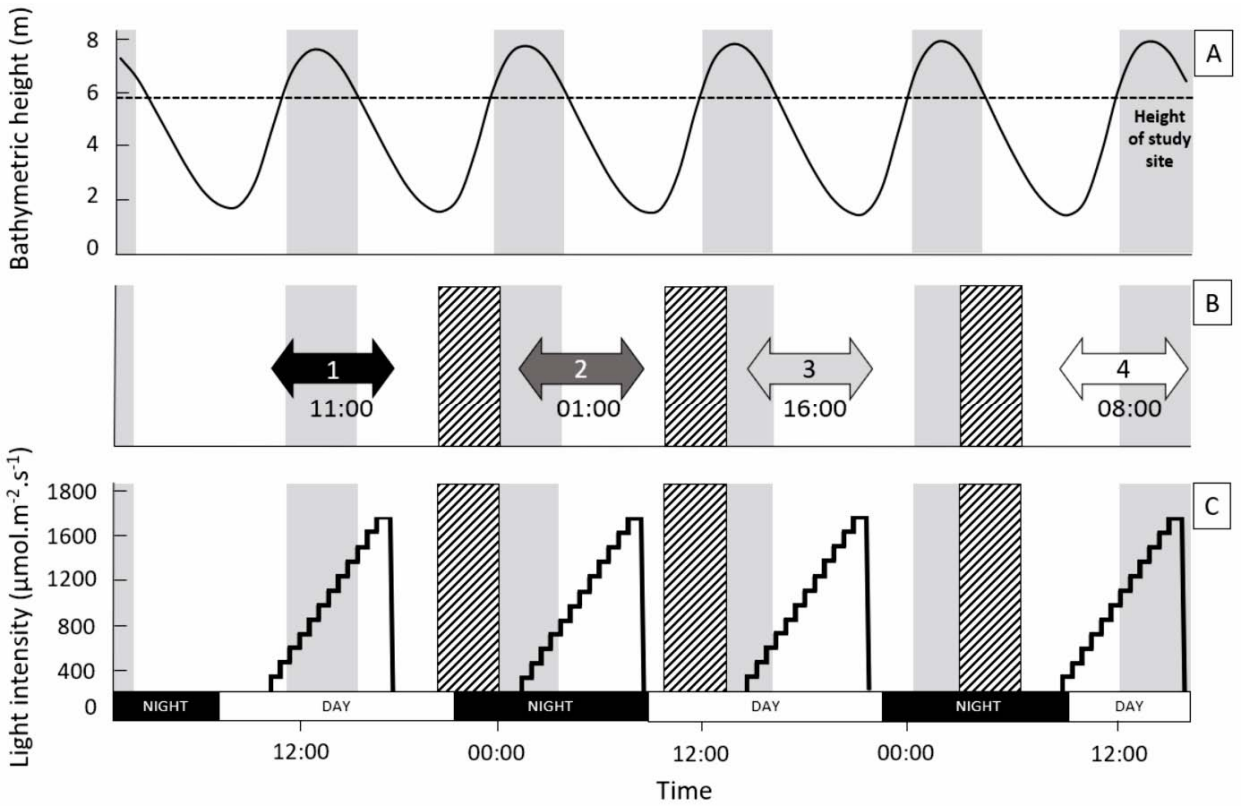

Figure 1. A: Tide evolution at the sampling site over time. The shaded areas represent the theoretical immersion phases. **B**: Diagram illustrating the artificial tidal cycle simulated in the laboratory. The numbered arrows (1 to 4) indicate the four scenarios during which measurement periods were conducted. The striped areas represent the immersion phases simulated in the laboratory. **C**: Evolution of the light intensity perceived by the microphytobenthos in the laboratory and the theorical alternance between day and night.

corresponding to an emersion comparable to that observed *in situ*. Thus, a total of 112 profiles were acquired for each scenario.

For this experiment, each profile was carried out down to a depth of 4.5 mm in order to systematically reach the anoxic layer, which corresponds to the depth where the microsensor signal reaches zero current (the depth of oxygen penetration). Oxygen partial pressure was converted to oxygen concentration as a function of measured surface sediment salinity and temperature [34].

Through the analysis of vertical oxygen microprofiles and utilization of the profiling software SensorTrace (Unisense, Denmark) numerical model, based on Berg *et al.*'s [35] model, an estimation of the net oxygen production (NOP) with depth was obtained. The model integrates various parameters, including the average porosity value measured within the first 5 millimeters, temperature, and salinity of the studied sediment. The NOP per unit area was estimated by vertically integrating production rates, assuming steady-state and 1D vertical exchanges, without considering irrigation and bioturbation processes. To determine fluxes attributable to the photosynthetic activity of the microphytobenthos in the sediment, the gross oxygen production (GOP) was calculated by subtracting the average oxygen flux values calculated in the dark from the NOP values obtained for each profile. In addition to exploiting the vertically integrated flux data, we also studied the evolution of the depth of oxygen concentration maximum (DOCM) in order to use it as a proxy for the depth of the maximum photosynthetic activity of the microphytobenthos (Figure 2).

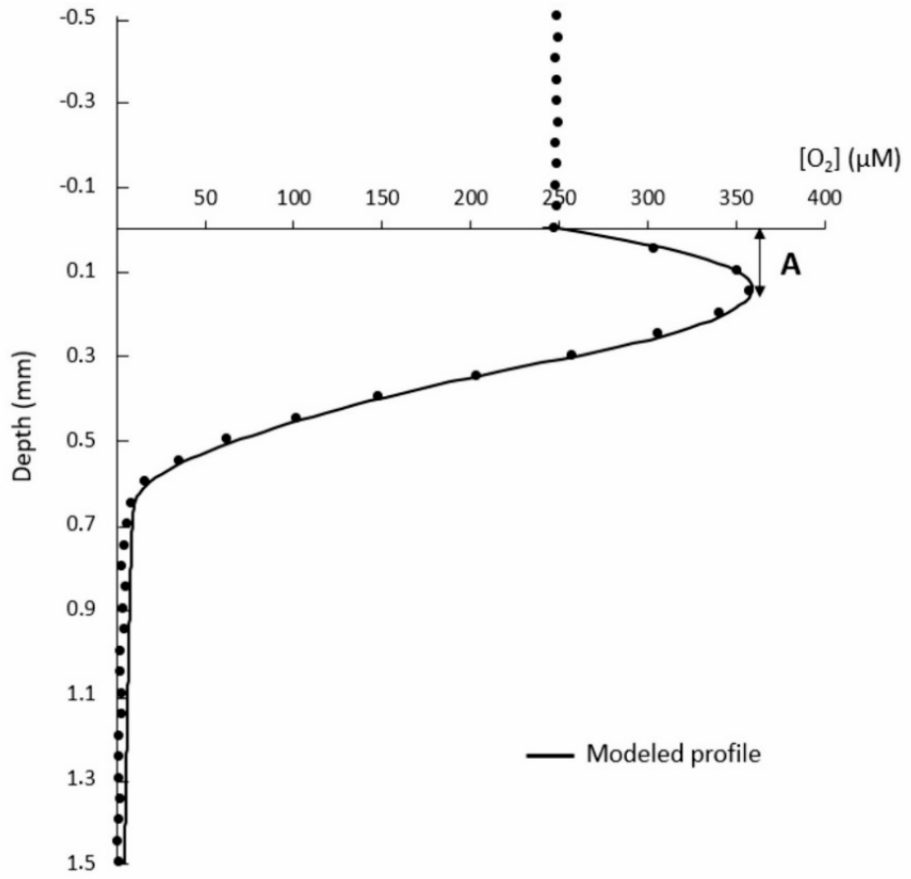

Figure 2. Raw oxygen concentrations measured under a light of 700 µmol.m^{-2}.s^{-1}. Distance A represents the depth of the maximum oxygen concentration.

2.2.2. Fluorescence measurement

Concurrently with the collection of vertical oxygen profiles, a diving-PAM fluorometer (Walz, Effeltrich, Germany) was employed to conduct variable fluorescence measurements every 3 minutes on the corresponding sediment core. This instrument allowed for the assessment of the effective quantum yield of photosystem II (PSII) (Φ_{PSII}). The calculation of Φ_{PSII} followed the equation developed by Genty *et al.* [36]:

$$\phi_{PSII} = \frac{F_m' - F_t}{F_m'} \quad (2)$$

where F_t represents the instantaneous fluorescence level under ambient light, while F_m' corresponds to the maximal level achieved with a single saturating light pulse (0.8 s, 2500 µmol.m^{-2}.s^{-1}) for light-acclimated samples. The relative electron transport rate (rETR) of photosystem II (PSII) under specific light intensities was calculated using Φ_{PSII} and the estimation method proposed by Genty *et al.* [36].

$$rETR = \phi_{PSII} \times PPFD \times 0.5 \quad (3)$$

The ambient light intensity, quantified as photosynthetic photon flux density (PPFD), was measured using a planar light sensor (LI-190, LICOR, Germany). The energy partitioning between the two photosystems was taken into account by using a factor of 0.5. The optimal quantum yield of PSII photochemistry (F_v/F_m) was used to evaluate the physiological condition of the microphytobenthic biofilm [36]. This parameter was calculated as the ratio:

$$\frac{F_v}{F_m} = \frac{F_m - F_0}{F_m} \quad (4)$$

where F_0 is the minimal fluorescence, and F_m is the maximal fluorescence attained during the application of a saturating pulse of white light (0.8 s, 2500 µmol.m^{-2}.s^{-1}), both levels measured after a period of 10 minutes in darkness. To ensure the accuracy of fluorescence measurements, the gain, damping, and intensity of the modulated light of the Diving-PAM were initially adjusted to achieve a minimum F_t value (>130) throughout the entire experiment. The fluorescence data presented in this study were averaged from 14 measurements obtained for each light intensity, ensuring reliable and representative results. Additionally, this parameter was measured both before and after the experimentation to assess any potential changes in the microphytobenthic biofilm.

2.3. P-I curve fitting and statistical analysis

The key photosynthetic parameters of the microphytobenthic communities, including the initial slope of the non-saturated photosynthetic rate (α) and the maximum production (P_{max}) [37, 38], were determined using statistical software R [39] and the Phytotools package (V1.0). The model proposed by Eilers and Peeters [40] was employed to estimate these parameters:

$$y = \frac{I}{\frac{I^2}{\alpha \times {I_k}^2} + \frac{I}{P_{max}} - \frac{2I}{\alpha \times I_K} + \frac{1}{\alpha}} \quad (5)$$

where y is the photosynthetic rate, I_k the optimal light intensity for primary production and I the photosynthetic photon flux density. To compare photosynthetic parameters, normality and homogeneity of variance were tested using the Shapiro-Wilk W-test, and results indicated non-normal distribution of the GOP data. Hence, non-parametric Wilcoxon tests were applied. The R statistical software was used to perform this statistical analysis.

Furthermore, to determine the periodicity of the fluorescence signal, the ‘sign’ function of R was used to calculate peak periods by defining the amplitude of the peak under study. As fluorescence data were not all of the same intensity from one experiment to another, the analysis was carried out on raw and normalized data.

3. Results

3.1. Sedimentary and biomass monitoring

Over a period of 5 consecutive days of sediment core conservation in artificial tide conditions, NOP measurements were conducted under four different light intensities. At dark, significant differences (P_{value}<0.05, n=20, Wilcoxon test) were observed in the measurements performed starting from the 4th day of maintenance. Under light conditions, significant differences were

observed from the 5th day onwards for low illumination of 200 µmol.m^{-2}.s^{-1}, and from the 4th day onwards for moderate illumination of 475 µmol.m^{-2}.s^{-1} and high illumination of 1020 µmol.m^{-2}.s^{-1} (Figure 3). Furthermore, profile analysis showed that the anoxic zone decreased from 764 ± 117 µm to 523 ± 78 µm (n=20) under equivalent light conditions.

To ensure that no settling of the sediment core occurred during the experiment, porosity of the first 0.5 cm of sediment was measured both before and after the simulation of the tidal cycle in the laboratory, with values varying from 0.81 ± 0.01 to 0.79 ± 0.03. No significant difference (P_{value}>0.05, n=6) was detected between the initial and final porosity values. Additionally, Chl *a* concentration was measured daily to ensure the preservation of the microphytobenthic communities. No significant difference appeared between the different days of experimentation (P_{value}>0.05, n=6). Furthermore, with a mean value of 0.58 ± 0.06 over the whole experiment, the F_v/F_m measurements revealed no significant differences between the various experimental days, both prior to and following the measurement sequence (P_{value}>0.05, n=6).

3.2. Fluorescence monitoring

The dynamics of the instantaneous surface fluorescence evolution are illustrated in Figure 4A. Distinct phases of both increasing and decreasing fluorescence can be observed. As the experiment progressed and the light intensity increased, a general decreasing trend in fluorescence can be observed. However, except for the last scenario, two noticeable increases in the fluorescence signal were observed: a prominently marked initial

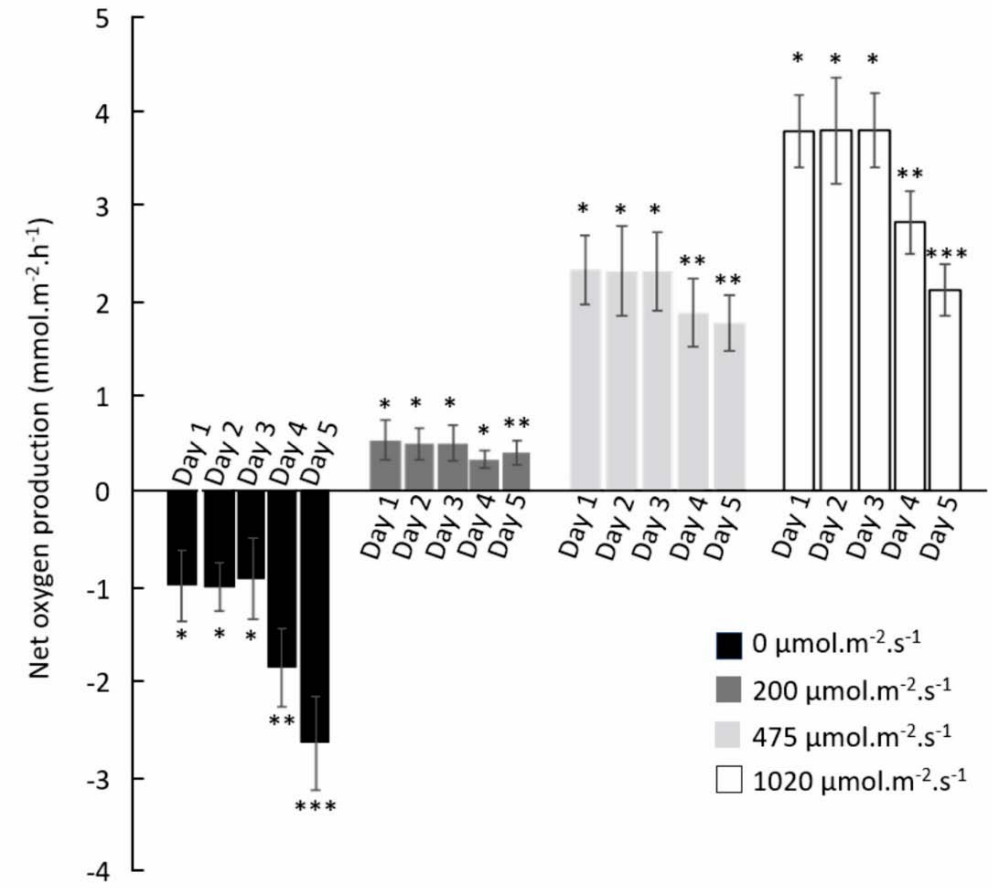

Figure 3. Net oxygen flux (mmol.m^{-2}.h^{-1}) (n=20 per day and light intensity) measured over 5 consecutive days at 4 different light intensities. Stars indicate whether the Wilcoxon test result is significant or not.

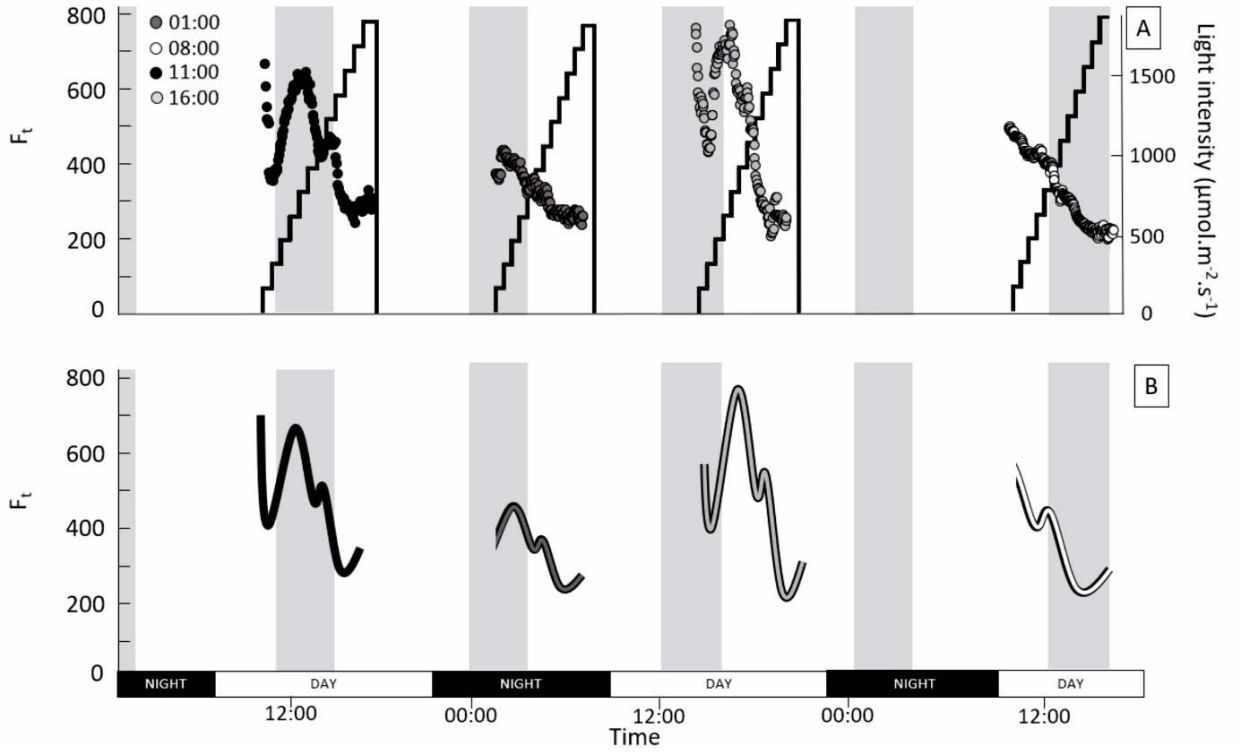

Figure 4. A: Instantaneous fluorescence dynamics (F_t) during the four scenarios according to the time, the tide (grey boxes) and the light. **B**: Fluorescence signal pattern obtained by smoothing.

increase followed by a second, less significant one.

The fluorescence evolution exhibited a redundant pattern across all scenarios, as depicted in Figure 4B. Although the patterns were identical, they differed in intensity depending on the specific scenario. In particular, the amplitudes of these patterns were 2.5 times greater in the daytime scenarios compared to the nighttime scenario. To study the redundancy of this pattern, a periodicity analysis of the data was conducted that revealed two distinct periods. The first period, calculated from the raw data, was found to be 25:20. Additionally, when analyzing normalized F_t data, a period of 13:03 ± 00:15 was identified.

3.3. P-I curves based on fluorescence measurements

Fluorescence measurements were used to calculate the relative electron transport rate (rETR). The P-I curves were modeled and are presented in Figure 5. The P-I curves revealed significant differences (P_{value}<0.05, n=6) in the maximum relative electron transport rate (rETR) between different scenarios with daytime and night-time measurements. Specifically, the 16:00 scenario exhibited an almost twofold higher maximum rETR compared to the 01:00 scenario, with the 08:00 and 11:00 scenarios falling in between these extremes (Figure 6A). On the other hand, no significant difference (P_{value}>0.05, n=6) was found between the 01:00 and the 08:00 α but these two alpha values are significantly lower than those of the 11:00 and 16:00 scenarios (Figure 6B).

3.4. P-I curves based on gross oxygen production

GOP integrated over the vertical of each profile were computed, and P-I curves were modeled by plotting these fluxes values according to light intensities for each hour of emersion (Figure 7). As the P-I curve was completed late in the day, the P_{max} was significantly higher (P_{value}<0.05, n=6) compared to nighttime conditions (Figure 8A). Moreover, there was a noticeable variation in P_{max} for P-I curves obtained during daylight hours,

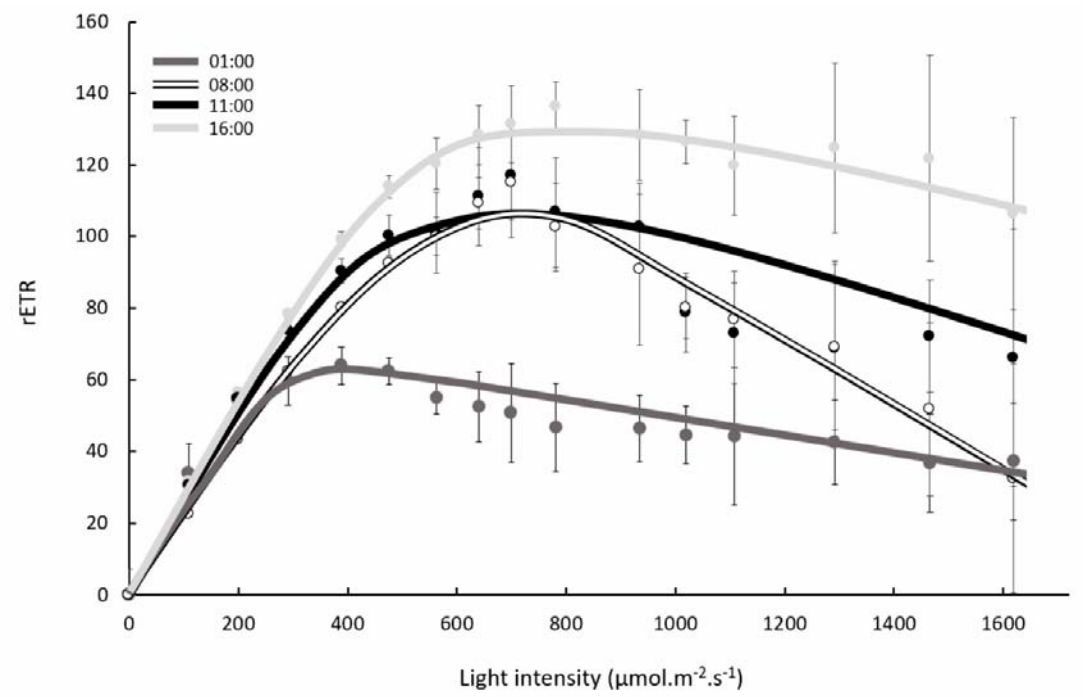

Figure 5. P-I curves obtained by fitting mean relative electron transport rate ± s.d (rETR) according to the light intensity (n=14), during the four scenarios, by using the model of Eilers and Peeters [40] (each point corresponds to the mean ± s.d).

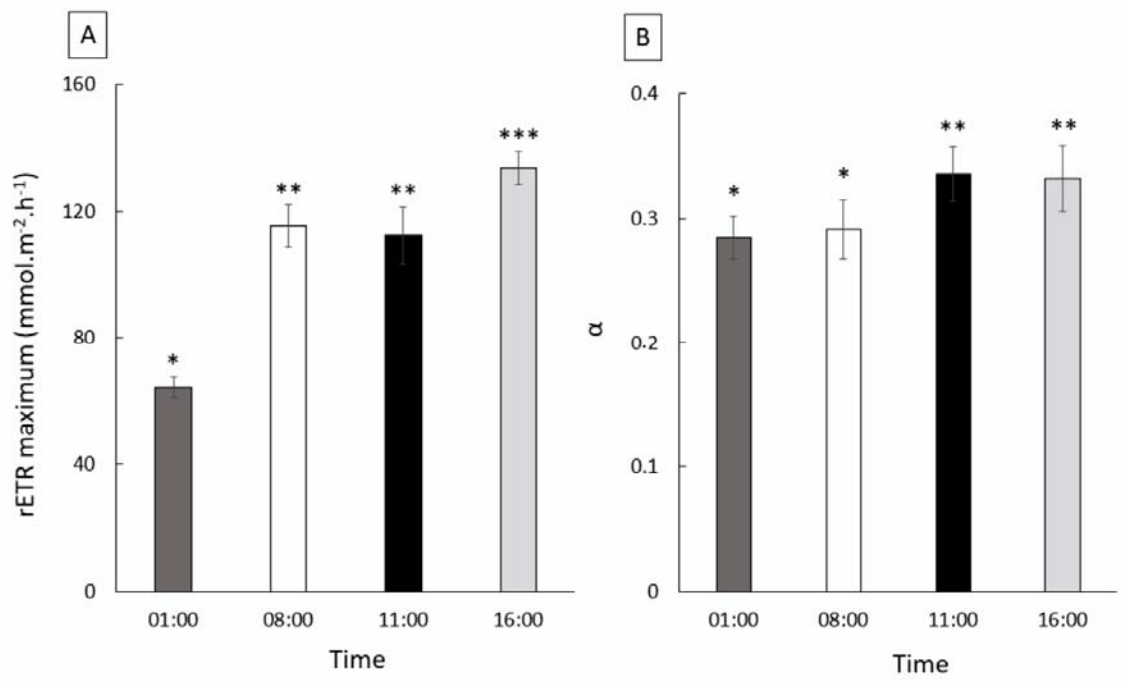

Figure 6. A: Mean value of α ± s.d. calculated on rETR P-I curves according to the scenario (n=12). **B**: Mean value of P_{max} ± s.d. calculated on rETR P-I curves according to the scenario (n=12). Stars indicate whether the Wilcoxon test result is significant or not.

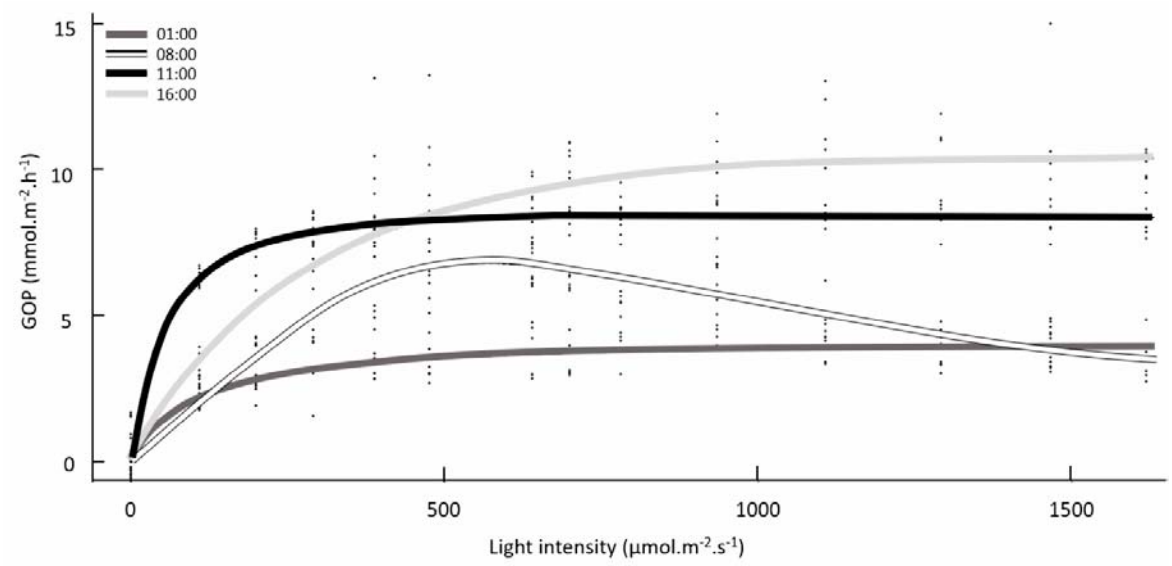

Figure 7. P-I curves obtained by fitting relative gross oxygen production according to the light intensity (n=6), during the four scenarios, by using the model of Eilers and Peeters [40].

with a significant increase of P_{max} values observed concurrently as the P-I curve was completed late in the day. Additionally, when immersions were simulated at 01:00 and 08:00, α values obtained were significantly lower (P_{value}<0.05, n=6) compared to the two others, with a five-fold increase in magnitude (Figure 8B). In the same way, α obtained at 16:00 was significantly lower (P_{value}<0.05, n=6) compared to the 11:00 one. Interestingly, under intense light conditions, a decrease in the GOP was observed, but this effect was only evident in the last scenario.

3.5. Depth of the oxygen concentration maximum

In order to get information about how the photosynthetic activity evolved vertically in the sediment, the DOCM is represented in Figure 9. In all scenarios, the depth of DOCM exhibited a tendency to increase initially, followed by either a decrease or stabilization under high light conditions, albeit to varying degrees. In addition, it is possible to observe that the amplitude of the DOCM varied across different scenarios with a lower magnitude for measurements made during the night compared to those taken during the day.

During the daytime scenarios (measurements starting at 11:00 and 16:00) the DOCM appeared to remain relatively stable when exposed to high light levels. Conversely, for scenarios carried out at 01:00 and 08:00, the DOCM showed less pronounced changes under high illumination.

Additionally, it is worth noting that in each experiment, a distinct change in slope could be observed during the transitions between the theoretical immersion and emersion phases of the study site. This observation becomes obvious when considering instances where the theoretical emersion occurred during daylight hours, irrespective of the light intensity (whether high or low). In such cases, there was a tendency for the DOCM to reach a stabilized state. This is also the case when the theoretical immersion occurred at night with a DOCM increasing initially under low light levels and then decreasing under high light levels. Finally, when the experiment concluded with theoretical immersion, the DOCM exhibited an instantaneous and linear decrease.

4. Discussion

4.1. Conservation of sediment cores in the laboratory

To assess the maximum feasible storage duration of a sediment core under laboratory conditions while simulating a tidal cycle, a preliminary experiment was conducted over a period of 5 consecutive days during the emersion phases of the artificial tidal cycle. The results of NOP

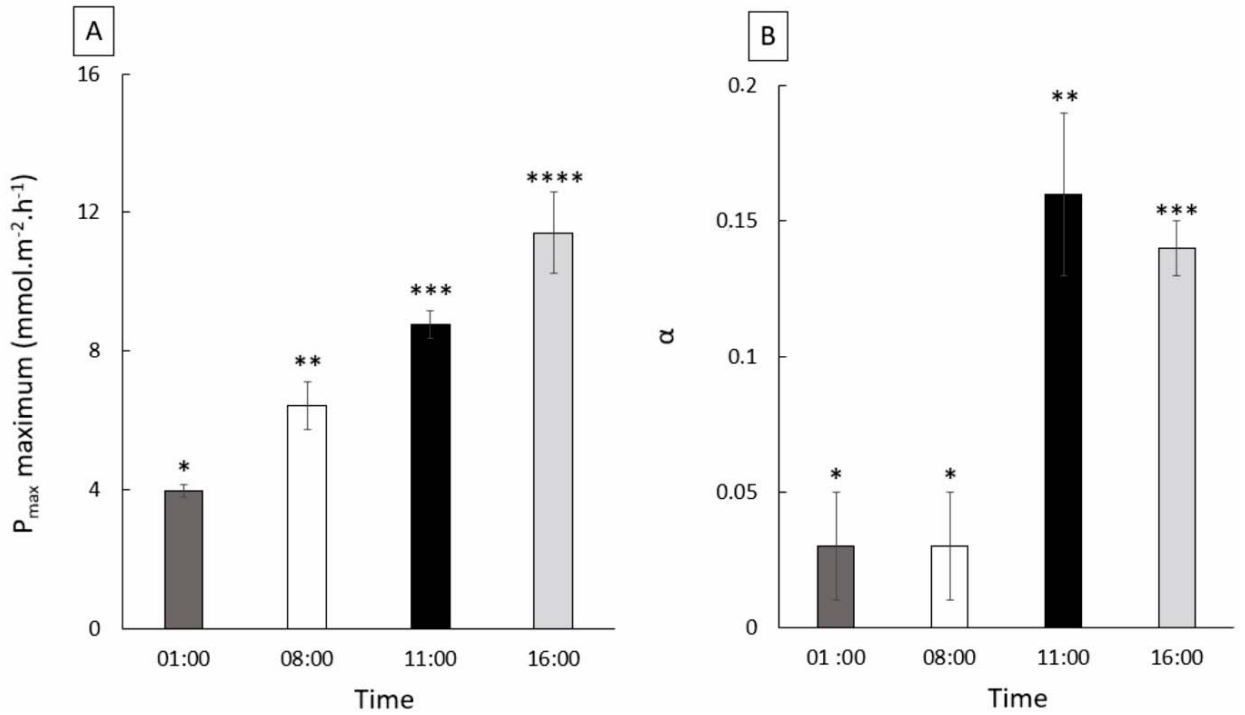

Figure 8. A: Mean value of α ± s.d. calculated on GOP P-I curves according to the scenario (n=6). **B**: Mean value of P_{max} ± s.d. calculated on GOP P-I curves according to the scenario (n=6). Stars indicate whether the Wilcoxon test result is significant or not.

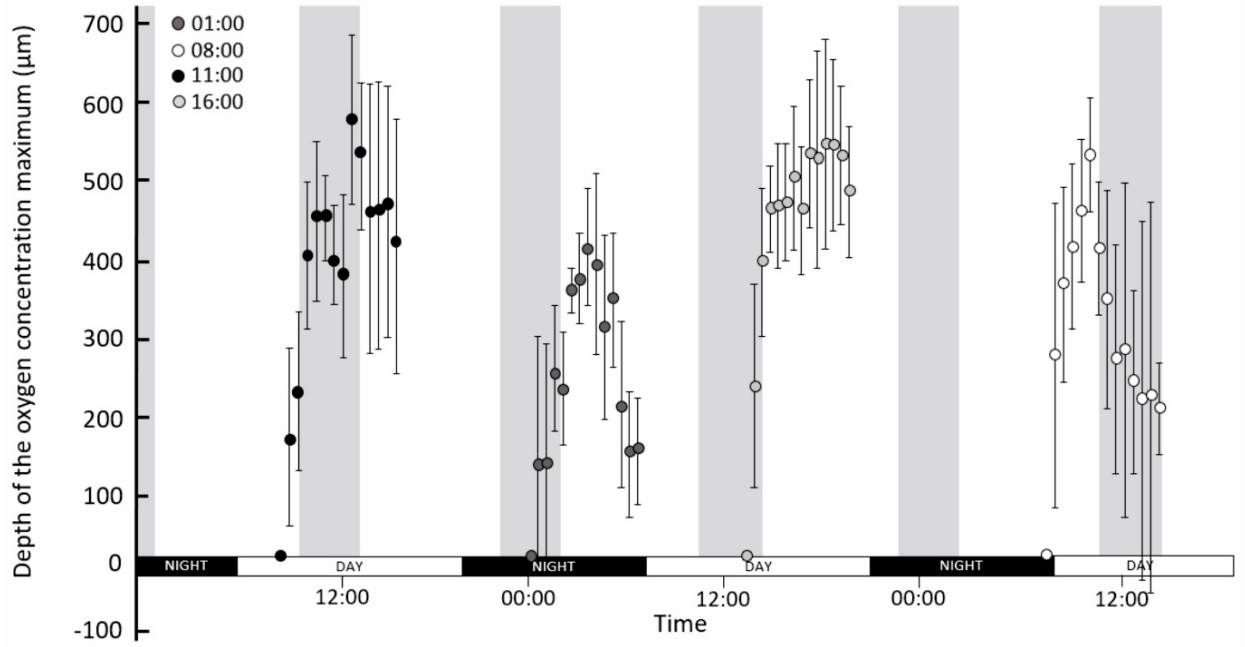

Figure 9. Average depth of oxygen concentration maximum ± s.d. (n=6) measured on oxygen profiles obtained during the four scenarios.

measurements revealed significant differences after 3 days of storage. Specifically, respiratory fluxes measured in the dark exhibited an increase, while NOPs measured under light conditions displayed a decrease. This alteration in oxygen fluxes can be attributed to the short life cycle of microphytobenthos cells [41]. Beyond 3 days, like *in situ,* a portion of the microphytobenthic community undergoes senescence, and the degradation of the biofilm could result in an accumulation of organic matter in the upper layers of the sediment. Due to the low mechanical disturbance caused by the absence of wave movement in the laboratory tidal simulation, this excess of organic matter could remain in the sediment rather than being flushed out. As a result, the increased organic matter content could have stimulated bacterial activity [42, 43], leading to heightened sediment respiration. This hypothesis finds support in the analysis of vertical profiles used for GOP calculations, where the average depth of the anoxic zone decreased from 764 ± 117 µm to 523 ± 78 µm (n=20) under equivalent light conditions.

As the sediment core was collected and stored under controlled conditions, we also ensured that this laboratory maintenance had no impact on the porosity of the sediment that could result from a compaction of the core during the 3 consecutive days of experiment. The average porosity of the first 0.5 cm before and after the three days of experimentation showed no significant differences with an average porosity of the studied sediment of 0.80 ± 0.02. This porosity value is quite close to the values observed in previous studies for the same site, with an average of 0.75 ± 0.02 in the study by Denis *et al.* [44], 0.90 ± 0.02 in the study by Denis *et al.* [45] or 0.92 ± 0.02 in the study by Meresse *et al.* [33]. With the same objective, a monitoring of the microphytobenthic biomass was carried out during the 3 days of experimentation for the first 5 surface millimeters through the measurement of Chl *a* concentration. No significant difference was found between the Chl *a* concentrations measured during the three days of experimentation, with an average concentration of 150.6 ± 9.50 $mg.m^{-2}$. This average value is however lower than the average concentrations found during the study of Denis *et al.* [45] and Meresse *et al.* [33] who measured an average concentration of 240 ± 30 and 270.93 ± 32.49 mg Chl *a*. m^{-2}, respectively during spring. This difference can be explained by temperature conditions that were lower in terms of seasonal averages. Thus, we can affirm that the conservation of the sediment cores in the laboratory during 3 days had no influence on the microphytobenthic biomass as well as on the porosity, which is the one of the main parameters taken into account in the calculation of the diffusive fluxes [46]. To finish, the F_v/F_m measurements exhibited no significant differences between experimental days, both before and after the measurement sequence. This indicates a consistent and stable physiological condition of the microphytobenthic communities throughout the duration of the study [36]. The average value obtained in this study for the F_v/F_m parameter is consistent with what is generally reported in the literature [47-50]. It is widely accepted that a F_v/F_m value above 0.7 indicates a good physiological state for photosynthetic organisms. However, for microphytobenthos, this F_v/F_m value is typically lower than 0.7 due to the positioning of the cells within the biofilm, which are not directly on the surface of the sediment but at its interface. As a result, the signal is attenuated by the interaction of the sediment between the microphytobenthos and the optical fiber of the fluorometer.

4.2. Impact of emersion hour on the microphytobenthic activity

4.2.1. Highlighting the internal clock

As for previous studies [19, 20, 22, 51], this experiment further elucidated the ability of microphytobenthos to exhibit an endogenous rhythm. By measuring F_t, we observed a consistent pattern over three consecutive days. The presence of the internal clock is further highlighted in our study through periodicity analyses, revealing two distinct periods: (i) a first period of 13:03 ± 00:15 minutes aligning approximately with a tidal cycle (in the English Channel, a tidal cycle occurs approximately every 12 hours and 45 minutes) and (ii) a second period of 25:20 corresponding to the tidal cycle plus the tidal shift, which includes a 24-hour cycle plus a 45-minute shift from one day to the next.

This slight discrepancy can be explained in our study by the fact that some factors, such as the life history of the microphytobenthos, need to be considered. During the days preceding the experiment, the mean atmospheric pressure was 1029 hPa (according to www.meteociel.fr), which is higher than the theoretical mean atmospheric pressure of 1013 hPa used in tidal forecasting models. It is possible that the microphytobenthos was synchronized to a different rhythm than the theoretical one due to the influence of atmospheric pressure, as it is known to affect water height [52].

While the internal clock mechanism has been previously demonstrated, to our knowledge, our study is the first to conduct oxygen fluxes and fluorescence measurements at different day and tide moment in order to reveal the importance of the moment of experimentation. Specifically, we observed that instantaneous fluorescence measurements were 2.5 times lower during nighttime measurements compared to daytime measurements. This suggests that microphytobenthos, through its internal clock, may regulate its migratory activity. Moreover, with variable maximum of P_{max} and maximum of rETR, microphytobenthos have demonstrated higher levels of photosynthetic activity during the day and lower levels at night, highlighting their ability to adapt their photosynthetic activity based on the time of day. The regulation of migratory behavior by their internal clock could play a crucial role in optimizing their light exposure and nutrient acquisition, ultimately influencing their overall ecological dynamics [53]. Like many other organisms, microphytobenthos has developed an internal clock, often referred to as a circadian and tide rhythm [18, 20, 22], which allows them to synchronize their biological activities with daily environmental changes. This internal timing mechanism allows them to anticipate and respond to environmental cues, such as changes in light availability [26] and nutrient availability [23], which are critical for their growth and survival. It ensures that these processes occur at the optimal time of day, maximizing their efficiency and resource utilization [23]. Like for numerous plant species [54], even if no studies have described this for microphytobenthos, the internal clock of microphytobenthos is thought to be governed by a molecular mechanism involving clock genes and proteins [55-57]. These clock genes produce proteins that interact in a feedback loop, creating oscillations in their expression levels over a 24-hour period [56]. This molecular feedback loop could allow microphytobenthos to maintain their internal timing and adjust their biological activities accordingly.

Beyond the variable photosynthetic activity between the different P-I curves, the variable intensity in the migratory activities of microphytobenthos, governed by the nychthemeral rhythm, can also be observed when considering the study of the DOCM. The trend observed in the depth of the migratory rhythm, as indicated by the DOCM, demonstrates variations corresponding to the nychthemeral rhythm. As already demonstrated thanks to F_t monitoring by Serôdio *et al.* [26], this study underscores the potential of utilizing the DOCM to demonstrate that, particularly during nighttime intervals, the migratory rhythm tends to occur at a mean depth of 413 ± 87 µm, while during the daytime, it shifts to a deeper average depth of around 581 ± 113 µm which means that, depending on the time of day, the depth at which photosynthetic activity is highest can vary, due to the intensity of migratory activity.

4.2.2. A life of ups and downs

By examining the patterns, it becomes apparent that there are distinct peaks that occur at different times of the day and tide. These peaks can be observed with varying degrees of intensity, indicating the presence of specific events or phenomena that contribute to the overall dynamics of the microphytobenthic communities.

In the 11:00 and 16:00 emersion scenario, a decrease in fluorescence values is observed. Since F_t measurements can serve as an indicator of microphytobenthic biomass, this decrease in surface signal suggests that the microphytobenthos is migrating into deeper layers of sediment. The mechanism behind this vertical migration towards deeper sediment layers can be attributed to the internal clock of the microphytobenthos. Despite being exposed to low light intensities, which would typically trigger vertical migration towards the surface [19, 58], the cells bury themselves

within the sediment in anticipation of the upcoming immersion period in the natural environment [18, 25]. This behavior enables to avoid the potential impact of the incoming tide and the resuspension caused by waves [25, 59]. By burrowing into the sediment, the microphytobenthos seeks to protect itself from these disturbances and ensure its survival and persistence within the intertidal zone. This mechanism has already been described in previous studies [28, 60] which have reported that the migratory movements of microphytobenthos typically occur within a time window of approximately 30 minutes before the transition between emersion and immersion and 30 minutes before flooding.

Following this downward migration, an increase and subsequent decrease in surface fluorescence were observed for the scenario of 11:00; 01:00 and 16:00 during the anticipated immersion phase. The increase in surface fluorescence could be attributed to the reemergence of the microphytobenthos from the deeper sediment layers as the theorical immersion period began. In many cases, when the study environment is turbid, the fluorescence signal does not increase on the surface during immersion phases [61, 62]. However, in this particular case, due to the experimental protocol that involved an increase in light intensity in the absence of tidal stimulus, positive phototaxis could trigger the migration of microphytobenthos towards the surface [26, 58, 63]. After a certain duration, these cells could experience excessive light intensity, which could lead to negative phototaxis and subsequent migration of the microphytobenthos back downwards [26, 63]. This migration behavior could be a response to optimize light exposure and avoid potential photodamage [26], highlighting the adaptive nature of microphytobenthic communities in responding to changes in light conditions. Furthermore, a second peak can be observed during the theoretical emersion period. This peak can be explained by an upward migration of microphytobenthic cells at the beginning of emersion because in turbid environments, during the time of theoretical emersion, microphytobenthos migrate towards the surface in order to capture light after a period of darkening induced by the tides [26, 58]. A second hypothesis may also explain this, since this peak is independent of tidal timing. It is possible that the microphytobenthic biofilm assemblage consists of species with different light preferences [58, 64]. Hence, the second peak could correspond to a second group of microphytobenthic cells emerging to the surface while the first group migrates downwards to reduce their exposure to light.

Lastly, in the 08:00 emersion scenario, a distinctive characteristic is observed where the theoretical immersion occurs at the end rather than the beginning. In this scenario, the fluorescence signal exhibits a single peak that occurs approximately 45 minutes prior to the theoretical immersion time. While previous studies have demonstrated the gradual loss of the endogenous rhythm in microphytobenthos [19, 22], the maintenance of the sediment core under artificial immersion and emersion conditions appears to preserve a certain degree of rhythmicity. This is evident from the observation of a noticeable break in slope in the fluorescence signal upon reaching the time of theoretical immersion. The presence of this break in slope suggests a shift in the dynamics of the microphytobenthic communities associated with the immersion phase. Despite the potential challenges posed by laboratory conditions, the experimental setup employed in this study has allowed for the preservation of rhythmic patterns in microphytobenthic behavior, providing valuable insights into the resilience and adaptability of these communities in response to artificially simulated immersion and emersion conditions.

4.2.3. A primary production controlled by the internal clock

The significance of this experiment lies in investigating the influence of the internal clock on the estimation of microphytobenthic primary productivity in laboratory settings. It is common to come across studies in the literature where the sampling protocol primarily involves collecting samples during low tide and subsequently transporting them to the laboratory for analysis [65, 66, 53]. However, this method presents certain challenges in terms of timing the experiments. Specifically, when conducting

experiments under emersion conditions, there are several considerations to address. Should the experiment begin immediately upon returning to the laboratory, without considering the ongoing processes in the natural environment? Should it be finished prior to the theoretical immersion at the collection site? Alternatively, should the experiment begin during the subsequent theoretical emersion phase? Furthermore, does the time of day pose any constraints on the experimental design? These questions highlight the complexities associated with studying microphytobenthos in laboratory settings and this can be seen in the P-I curves obtained from GOP measurements.

Through the acquisition of four GOP P-I curves in different scenarios, it becomes evident that the time of day exerts an influence on the estimation of primary production. When conducting P-I curves during nighttime, despite standard experimental conditions across all scenarios, the maximum production is lower compared to other scenarios. As the P-I curve measurements are conducted later in the day, there is an increase in P_{max}, with the 16:00 scenario demonstrating approximately twice the maximum production compared to the 01:00 scenario. These findings indicate that the time of day plays a role in shaping the primary production estimates. This phenomenon can be attributed to the ability of microphytobenthos to modulate its photosynthetic activity through its internal clock. Like for GOP, when examining the P-I curves obtained through rETR measurements, a discernible increasing gradient of photosynthetic activity throughout the day is observed, with the 16:00 scenario exhibiting a maximum rETR approximately twice as high as the 01:00 scenario. This highlights the dynamic nature of microphytobenthic photosynthetic activity and its responsiveness to diurnal variations, underscoring the importance of considering time of day as a contributing factor when assessing primary production in laboratory experiments.

In addition to the day/night effect on the intensity of photosynthetic activity in microphytobenthos, the increasing trend in P_{max} as the P-I curve is completed later in the day can be attributed to the microphytobenthic light history. Indeed, the physiological state of microphytobenthic communities is a key factor in its photosynthetic capacity [53, 67, 68]. According to the hour of the day, it is possible that their metabolic activity and readiness for photosynthesis increase over the course of the day, leading to higher P_{max} values. By conducting the scenario at 16:00, the microphytobenthos experiences optimal conditions for photosynthesis. During an emersion in the mid-afternoon, the microphytobenthos has already passed through the most challenging period in terms of light intensity, as it was in darkness. Being immersed at the time of the sun's zenith, it is less prone to photoinhibition. Moreover, prior to the zenith immersion, the microphytobenthos has been exposed to low light levels, which are considered optimal for growth [69, 70]. Therefore, from a productivity standpoint, it appears that an afternoon emersion is the most effective.

Similarly, conducting an emersion at 11:00 will also have an impact on the photosynthetic response of the microphytobenthos due to its light history. Before this emersion, the microphytobenthos will have experienced darkness during the previous night and low light intensities during early morning. This resting period allows the light-harvesting antennae to adapt to low light levels, optimizing their ability to capture light [71]. As a result, the microphytobenthos will exhibit a higher α value compared to the other daytime experiments resulting in a more efficient photosynthetic capacity under low light levels [72-74]. By analyzing alpha values on the P-I curves derived from rETR and GOP data, we observe no substantial difference between α values obtained from the 11:00 and 16:00 curves in the fluorescence data. This lack of significant difference could be attributed to the fact that rETR is calculated based on surface measurements. Consequently, it is plausible that biofilm cells with reduced migratory abilities might not be detected at lower light levels, leading to distinguishable slopes when comparing surface and depth-integrated measurements.

Finally, when studies begin at 08:00, microphytobenthos communities have remained unexposed to light from the sunset time until measurement time. Moreover, the microphytobenthos benefited from the previous afternoon's emersion, during which it experienced high photosynthetic activity. It is plausible to suggest that during

this period, metabolic reserves were replenished, reducing the immediate need for intense photosynthetic activity and migratory behavior because microphytobenthos can rely on the stored metabolic reserves during this time, optimizing resource allocation and energy utilization for its physiological processes. To our knowledge, no study has been carried out on microphytobenthic capacity to stock metabolites, but some studies have already been done on other pelagic species of diatoms [75]. This may explain why the P_{max} value at 08:00 is lower compared to scenarios where the microphytobenthos experienced different light histories. Furthermore, the P-I curve obtained in this scenario is the only one where photoinhibition can be observed. There are two possible explanations for this: (i) as the experiment approaches three consecutive days, as Serôdio [22] has shown, the endogenous rhythm is lost, or (ii) given the experimental design, it is possible that performing GOP measurements at high light intensities during a theoretical immersion phase could disturb the microphytobenthos. From the DOCM, it can be observed that the maximum production depth appears to rise towards the surface during the theoretical immersion period. This could indicate that the microphytobenthos undergoes a subsurface migration towards the surface in response to the internal clock, but without actually reaching the surface, resulting in photoinhibition due to excessively high light levels.

CONCLUSIONS

This study confirms that microphytobenthos in intertidal zones maintains an endogenous rhythm through an internal clock that remains functional even under laboratory conditions. Additionally, it highlights the importance of considering the time of day during laboratory measurements. Results demonstrate that, even under controlled and standardized conditions, microphytobenthic photosynthetic response can vary significantly depending on both the time of day and the theoretical tidal phase, highlighting the importance of considering time of day and tide when performing P-I curve experiments in laboratory. For future experiments, it would be valuable to investigate the underlying mechanisms and determine the duration required for the complete loss of this internal clock without impacting the physiological capacities of microphytobenthos. Understanding these aspects would provide further insights into the temporal dynamics and adaptive capabilities of microphytobenthos in intertidal ecosystems.

ACKNOWLEDGEMENTS

We thank Marine Doublet for her participation in the laboratory experiments during her Master's internship.

AUTHOR'S CONTRIBUTIONS

Conceptualization, MM; Data curation, MM, FG, GD and LD; Formal analysis, MM, FG and LD; Methodology, MM, FG and LD; Supervision, FG and LD; Writing—review and editing, MM, FG and LD. All authors contributed to the article and approved the submitted version.

CONFLICT OF INTEREST STATEMENT

The authors declare that the research was conducted in the absence of any commercial or financial relationships that could be construed as a potential conflict of interest.

ABBREVIATIONS

Φ_{PSII}	:	Effective quantum yield of photosystem II
ρ_{sed}	:	Dry particle density
ρ_w	:	Seawater density
α	:	Initial slope of the non-saturated photosynthetic rate
Chl *a*	:	Chlorophyll *a*
DOCM	:	Depth of Oxygen Concentration Maximum
F_0	:	Minimal fluorescence for dark-adapted samples
F_m	:	Maximal fluorescence level achieved with a single saturating light pulse
F_m'	:	Maximal fluorescence level achieved with a single saturating light pulse for light-acclimated samples
F_t	:	Instantaneous fluorescence level under ambient light
F_v/F_m	:	Optimal quantum yield of PSII photochemistry

GOP	:	Gross Oxygen Production
I_k	:	Optimal light intensity for primary production
NOP	:	Net Oxygen Production
PAM	:	Pulse-amplitude modulated
P-I curve	:	Photosynthetic-Irradiance curve
PPFD	:	Photosynthetic Photon Flux Density
P_{max}	:	Maximum of primary production
PSII	:	Photosystem II
rETR	:	relative Electron Transport Rate
W_{sed}	:	Sediment weight
W_w	:	Water weight
y	:	Photosynthetic rate

REFERENCES

1. Hume, T. M., Bell, R. G., de Lange, W. P., Healy, T. R., Hicks, D. M. and Kirk, R. M. 1992, N. Z. J. Mar. Freshwater Res., 26, 1.
2. Hopkinson, C. S., Giblin, A. E., Tucker, J. and Garritt, R. H. 1999, Estuaries, 22, 863.
3. Admiraal, W. 1984, Prog. Phycol. Res., 3, 269.
4. MacIntyre, H. L., Geider, R. J. and Miller, D. C. 1996, Estuaries, 19, 186.
5. Underwood, G. J. C. and Kromkamp, J. 1999, Adv. Ecol. Res., 29, 93.
6. Sundbäck, K. 1984, Ophelia, 3, 229.
7. Cariou, V. 1995, Mar. Ecol. Prog. Ser., 121, 171.
8. Guarini, J. M., Blanchard, G. F., Bacher, C., Gros, P., Riera, P., Richard, P., Gouleau, D., Galois, R., Prou, J. and Sauriau, P. G. 1998, Mar. Ecol. Prog. Ser., 166, 131.
9. Cahoon, L. B. 2006, Functioning of microphytobenthos in estuaries, J. Kromkamp (Ed.), Amsterdam, 99.
10. Christianen, M., Middelburg, J. J., Holthuijsen, S., Jouta, J., Compton, T., van der Heide, T., Piersma, T., Sinninghe Damsté, J. S., van der Veer, H. and Schouten, S. J. 2017, Ecology, 98, 1498.
11. Hanelt, D., Huppertz, K. and Nultsch, W. 1993, Mar. Ecol. Prog. Ser., 97, 31.
12. Coelho, H., Vieira, S. and Serôdio, J. 2009, J. Exp. Mar. Biol. Ecol., 381, 98.
13. Kirst, G. O. 1989, Annu. Rev. Plant Physiol. Plant Mol. Biol., 40, 21.
14. Le Rouzic, B. 2012, Estuar. Coast. Shelf. Sci., 115, 326.
15. Cohn, S. A., Dunbar, S., Ragland, R., Schulze, J., Suchar, A., Weiss, J. and Wolske, A. 2016, Diatom Res., 31, 173.
16. Apoya-Horton, M. D., Yin, L., Underwood, G. J. C. and Gretz, M. R. 2006, J. Phycol., 42, 379.
17. Paterson, D. M. 1986, Diatom Res., 1, 227.
18. Coelho, H., Vieira, S. and Serôdio, J. 2011, Eur. J. Phycol., 46, 271.
19. Barnett, A., Méléder, V., Dupuy, C. and Lavaud, J. 2020, Front. Mar. Sci., 7, 212.
20. Haro, S., Bohórquez, J., Lara, M., Garcia-Robledo, E., González, C. J., Crespo, J. M., Papaspyrou, S. and Corzo, A. 2019, Sci. Rep., 9. 13376.
21. Palmer, J. D. and Round, F. E. 1967, Biol. Bull., 132, 44.
22. Serôdio, J., da Silva, J. M. and Catarino, F. 1997, J. Phycol., 33, 542.
23. Serôdio, J. 2021, Diatom Gliding Motility, S. A. Cohn, K. M. Manoylo and R. Gordon (Eds.), Wiley-Scrivener, Beverly, 159.
24. Saburova, M. A. and Polikarpov, I. G. 2003, Mar. Ecol. Progr. Ser., 251, 115.
25. Consalvey, M., Paterson, D. M. and Underwood, G. J. C. 2004, Diatom Res., 19, 181.
26. Serôdio, J., Bastos, A., Morelle, J. and Frankenbach, S. 2023, Ecol. Modell., 481, 110379.
27. Jesus, B., Brotas, V., Ribeiro, L., Mendes, C. R., Cartaxana, P. and Paterson, D. M. 2009, Cont. Shelf Res., 29, 1624.
28. Paterson, D. M., Wiltshire, K. H., Miles, A., Blackburn, J. and Davidson, I. 1998, Limnol. Oceanogr., 43, 1207.
29. Lorenzen, C. J. 1967, Limnol. Oceanogr., 12, 343.
30. Danovaro, R., Marrale, D., Della Croce, N., Parodi, P. and Fabiano, M. 1999, J. Sea. Res., 42, 117.
31. Flemming, B. W. and Delafontaine, M. T. 2000, Cont. Shelf. Res., 20, 1179.
32. Mackin, J. E. and Aller, J. C. 1984, Limnol. Oceanogr., 29, 250.
33. Meresse, M., Gevaert, F., Duong, G. and Denis, L. 2023, Front. Mar. Sci., 10, 3389.
34. Garcia, H. E. and Gordon, L. I. 1992, Limnol. Oceanogr., 37, 1307.

35. Berg, P., Risgaard-Petersen, N. and Rysgaard, S. 1998, Limnol. Oceanogr., 43, 1500.
36. Genty, B., Briantais, J. M. and Baker, N. R. 1989, Biochim. Biophys. Acta Gen. Subj., 990, 87.
37. Coutinho, R. and Zingmark, R. 1987, J. Phycol., 23, 336.
38. Henley, W. J. 1993, J. Phycol., 29, 729.
39. R Core Team, 2017, A language and environnement for statistical computing, Vienna, available at: https://www.R-project.org/
40. Eilers, P. H. C. and Peeters, J. C. H. 1988, Ecol. Modell., 42, 199.
41. Mann, D. G. 1989, The chromophyte algae: Problems and perspectives, J. C. Green (Ed.), Oxford, 307.
42. Hargrave, B. T. 1972, Limnol. Oceanogr., 17, 583.
43. Middelburg, J. J., Vlug, T. and van der Nat, F. W. A. 1993, Global Planet Change, 8, 47.
44. Denis, L. and Desreumaux, P. E. 2009, Mar. Freshw. Res., 60, 712.
45. Denis, L., Gevaert, F. and Spilmont, N. 2012, J. Soils Sediments, 12, 1517.
46. Boudreau, B. P. and Jørgensen, B. 2001, The Benthic Boundary Layer: Transport Processes and Biogeochemistry, B. P. Boudreau and B. B. Jorgensen (Ed.), Oxford, 211.
47. Serôdio, J., Cruz, S., Vieira, S. and Brotas, V. 2005, J. Exp. Mar. Biol. Ecol., 326, 157.
48. Serôdio, J., Vieira, S., Cruz, S. and Barroso, F. 2005, Mar. Biol., 146, 903.
49. Jesus, B., Brotas, V., Marani, M. and Paterson, D. M. 2005, Estuar. Coast. Shelf. Sci., 65, 30.
50. Du, G. Y. and Chung, I. K. 2009, Ocean Sci. J., 44, 189.
51. Serôdio, J., Vieira, S. and Cruz, S. 2008, Cont. Shelf Res., 28, 1363.
52. Hamon, B. V. 1966, J. Geophys., 71, 2883.
53. Cartaxana, P., Cruz, S., Gameiro, C. and Kühl, M. 2016, Front. Mar. Sci., 7, 872.
54. Yakir, E., Hilman, D., Harir, Y. and Green, R. M. 2006, FEBS J., 274, 335.
55. Millar, A. 2003, J. Exp. Bot., 55, 277.
56. Foster, R. G. and Kreitzman, L. 2014, Exp. Physiol., 99, 559.
57. Ronald, J. and Davis, S. J. 2017, F1000Res., 6, 951.
58. Laviale, M., Frankenbach, S. and Serôdio, J. 2016, Mar. Biol., 160, 10.
59. Hopkins, J. T. 1963, J. Mar. Biol. Assoc. UK, 43, 653.
60. de Brouwer, J. F. C. and Stak, L. J. 2001, Mar. Ecol. Progr. Ser., 218, 3344.
61. Daggers, T. D., Kromkamp, J. C., Herm, P. M. J. and Van Der Wal, D. 2018, Remote Sens. Environ., 211, 129.
62. Frankenbach, S., Ezequiel, J., Plecha, S., Goessling, J. W., Vaz, L., Kühl, M., Dias, J. M., Vaz, N. and Serôdio, J. 2020, Front. Mar. Sci., 7, 1.
63. Longphuirt, S. N., Leynaert, A., Guarini, J. M., Chauvaud, L., Claquin, P., Herlory, O., Amice, E., Huonnic, P. and, Ragueneau, O. 2006, Mar. Ecol. Progr. Ser., 328, 143.
64. Mouget, J., Perkins, R., Consalvey, M. and Lefebvre, S. 2008, Aquat. Microb. Ecol., 52, 223.
65. Brotas, V. and Catarino, F. 1995, Neth. J. Aqua. Ecol., 29, 333.
66. Blanchard, G. F., Guarini, J. M., Gros, P. and Richard, P. 2008, J. Phycol., 33, 723.
67. Chevalier, E., Gevaert, F. and Créach, A. 2010, J. Exp. Mar. Biol. Ecol., 385, 44.
68. Salleh, S. and McMinn, A. 2022, J.M.B.A., 102, 425.
69. McMinn, A. and Lee, S. 2018, J. Phycol., 54, 410.
70. Montani, S., Magni, P. and Abe, N. 2003, Mar. Ecol. Progr. Ser., 249, 79.
71. Guenther, J. E., Nemson, J. A. and Melis, A. 1988, Biochim. Biophys. Acta, 934, 108.
72. Green, R. M., Geider, R. J. and Falkowski, P. G. 1991, Limnol. Oceanogr., 36, 1772.
73. Geider, R. J., La Roche, J., Greene, R. M. and Olaizola, M. 1993, J. Phycol., 29, 755.
74. Falkowski, P. G. and Kolber, Z. 1995, Aust. J. Plant. Physiol., 22, 341.
75. Lancelot, C. and Mathot, S. 1985, Mar. Biol., 86, 219.